Investigation of the quality of the groundwater and the nitrate pollution hazards to human health in the desert region of Algeria.

Alia Sara Lakhdari [1,] Boualem Bouselsal *[1]

[1.]Laboratory of Underground Oil, Gas and Aquifer Reservoirs, Department of Earth and Universe Sciences, University of Kasdi Merbah, Route de Ghardaïa, Ouargla, Algeria

***Corresponding author email:** bouboualem@gmail.com

Received: 03 April 2024 / Accepted: 13 August 2024

Abstract Groundwater in the desert zone is important for supporting all life forms in these regions. This research focused on analyzing the quality of groundwater and the threats posed by nitrate contamination in the Continental Intercalary Aquifer (CI) in the Adrar region. Twenty-five groundwater samples were collected and assessed for pH, electrical conductivity, and major ions, employing hydrochemical diagrams, multivariate statistical analysis, and indices such as the Pollution Index of Groundwater (PIG), Nitrate Pollution Index (NPI), and Health Risk Assessment (HRA).The findings revealed the typical order of ion concentrations: $Na^+ > Ca^{2+} > Mg^{2+} > K^+$ for cations and $Cl^- > SO_4^{2-} > HCO_3^- > NO_3^-$ for anions. These concentrations result from natural processes like evaporation and the dissolution of evaporites, along with anthropogenic influences, primarily from agricultural and urban sources. The PIG values categorized 28% of samples as having insignificant pollution, 48% as low, and 24% as high. Moreover, NPI results showed that 24% of samples had insignificant pollution, 44% displayed mild pollution, and 32% were moderately polluted. The Health Risk Assessment highlighted significant non-carcinogenic risks due to nitrate exposure. Hazard quotient values exceeded the safe threshold of 1 in 80% of samples for infants, 76% for children, and 64% for adults, indicating significant health risks. These findings underscore the critical need for targeted treatment strategies to ensure safe drinking water for the region's population. This comprehensive analysis demonstrates the critical interplay between natural and human factors in shaping groundwater quality and emphasizes the importance of continued monitoring and intervention to protect public health.

Keywords: Groundwater of the desert zone, Multivariate analyses, Groundwater Pollution Index, Health risk assessment, nitrate contamination.

1. Introduction

The fundamental role of fresh water in the rise and support of civilizations throughout history is undeniable. From the beginnings of the earliest human communities settled near water sources, to the current era characterized by advanced societies, water has always been a key element, proving crucial for combating poverty, ensuring food security, and promoting sustainable development. Among fresh water reserves, groundwater stands out as the main source after glaciers, playing a vital role in human survival and social progress (Gleick, 2003). With nearly 2.5 billion people exclusively depending on groundwater for their daily needs, the significance of this resource for access to drinking water and the support of agricultural and industrial sectors is evident (UNESCO, 2012). However, this precious resource is now threatened by depletion and the degradation of its quality due to factors such as population growth, agricultural expansion, industrialization, and climate change, challenges that are accentuated in arid and semi-arid areas (Foster et al., 1997; Massuel et al., 2013).

The Adrar area, located in an arid region and part of the North Sahara aquifer system, contains significant groundwater reserves, stored in permeable geological formations dating from the Lower Cretaceous and known as the Continental Intercalary (CI) aquifer (UNESCO, 1972; Benhamida, 2020; Darling et al., 2018). This resource constitutes the only source of water available in the region, but its increasing exploitation for human consumption and irrigation has led to multiple overuse problems, including groundwater level reduction, deterioration of water quality, and pollution from irrigation and wastewater, with alarming levels of dissolved salts and nitrates often exceeding potability standards (WHO, 2017; USEPA, 1989).

Facing these challenges, understanding nitrate contamination in groundwater is crucial for preventing risks to human health and ensuring a quality drinking water supply. Therefore, this study aims to explore (1) the physico-chemical characteristics of the CI aquifer water, (2) the hydrochemical processes influencing its composition and the origin of nitrates, (3) contamination levels and their compliance for consumption, as well as (4) the impact of nitrate pollution on the health of the Adrar population. Methods used include multivariate statistical analysis, the Pollution Index of Groundwater (PIG), the Nitrate Pollution Index (NPI), and the Health Risk Assessment (HRA) following the computational methodology proposed by the USEPA (USEPA, 1989; Adimalla, 2020a; Subba Rao et al., 2021; Kharroubi et al., 2024). The methodology of this research is illustrated in Figure 1.

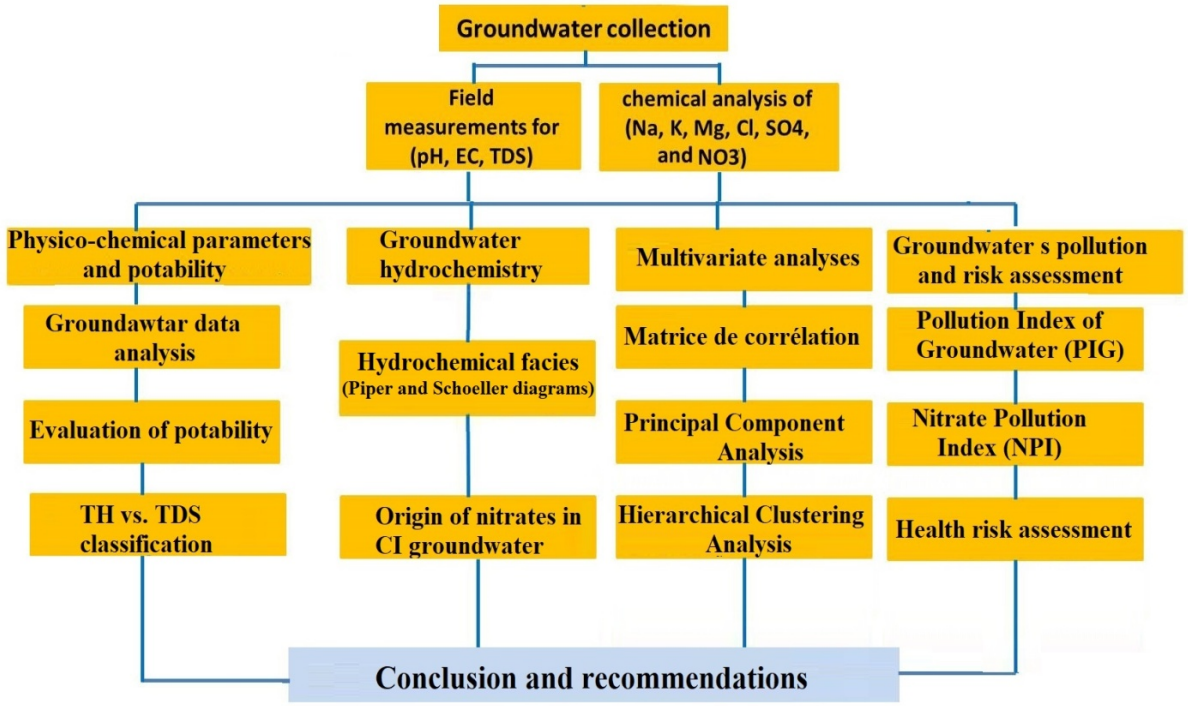

Figure 1. Methodological flowchart for this study.

2. Study area

The study area is situated in Adrar Province, located in the southwest of Algeria, at the center of the Sahara region (Fig. 2). Covering an area of 540 km^2, it has a population of approximately 90,000. The region is geographically defined within the UTM-WGS84 coordinate system, extending from east longitudes 75,000 to 780,000 and north latitudes 3,070,000 to 3,102,500. Adrar is characterized by an extremely arid climate, with average annual precipitation of about 9.50 mm and evapotranspiration of approximately 2700 mm/year. This combination of low precipitation and high evapotranspiration results in a significant water deficit, typical of desert climates.

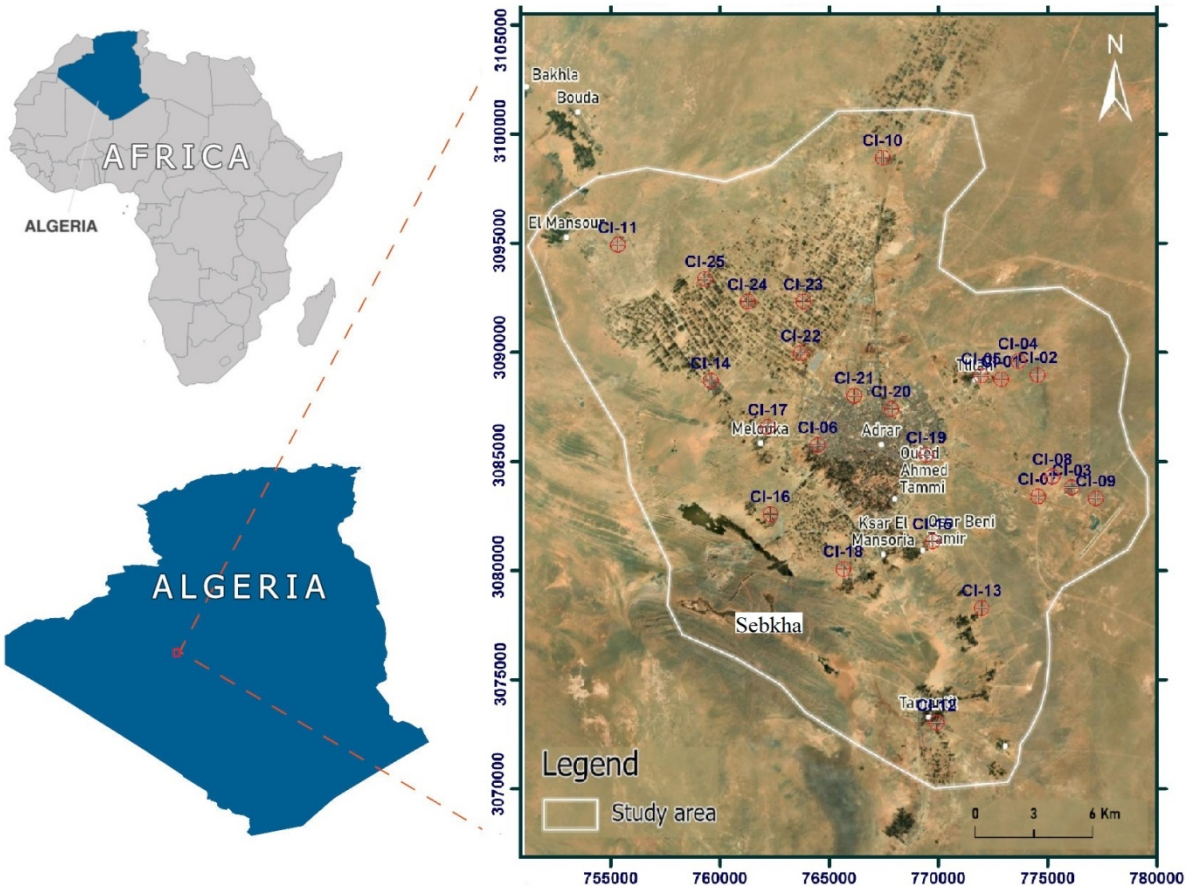

Figure 2. Situation map and inventory of water samples analyzed.

From a geomorphological perspective, the study region exhibits several distinctive characteristics. It is primarily defined by the Reg, a flat, gravelly expanse, interspersed with rocky remnants and bordered by imposing dunes to the west. The altitudinal gradient of this region gradually decreases from northeast to southwest (Fig. 3), leading to a depressive area. This depression is occupied by a Sebkha, located downstream from the Adrar palm grove, illustrating the dynamic interaction between landforms and local ecosystems.

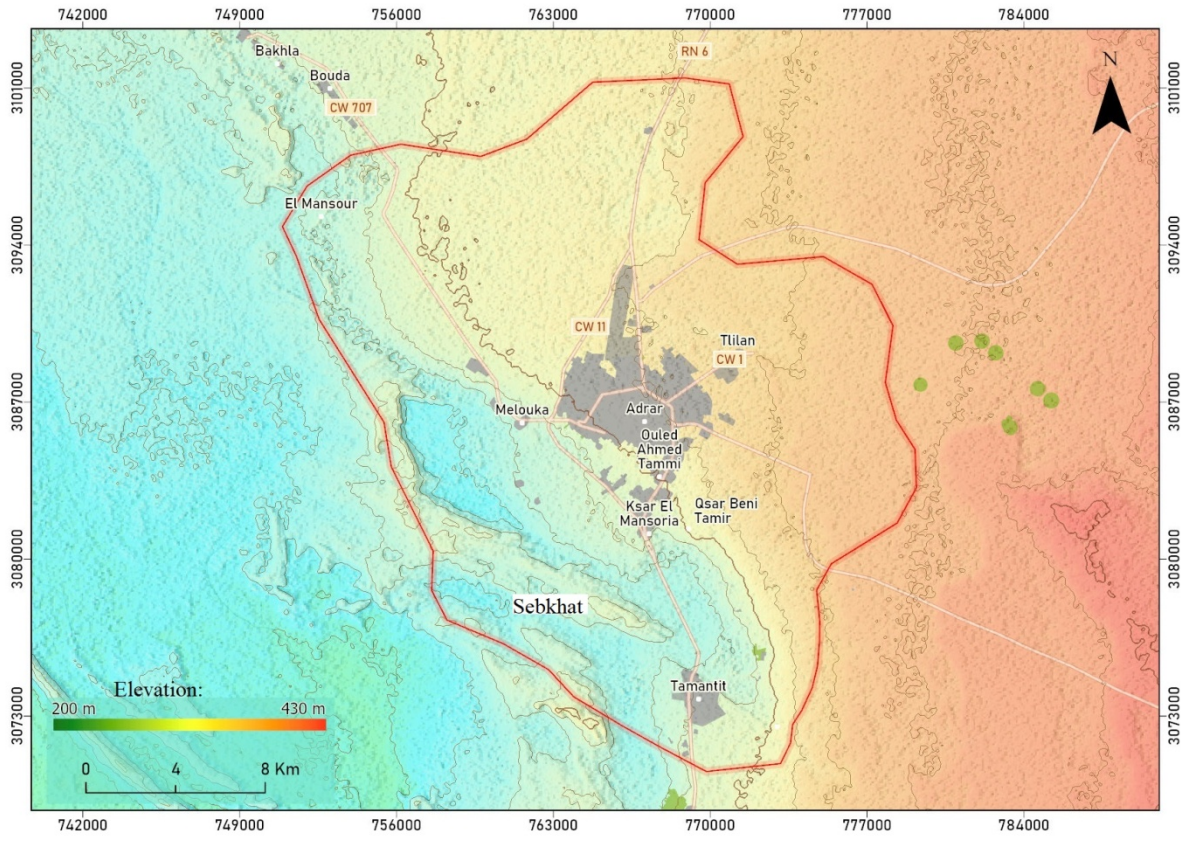

Figure 3. Map of the elevation variation in the study area.

From a geological perspective, the study area is situated within the large Saharan platform, part of the North African Craton. It consists of a Precambrian basement overlain discordantly by a thick sedimentary cover (Boualem and Egbueri, 2024; Benhamida, 2020; Darling et al., 2018). The primary formations, or Paleozoic, are mainly composed of sandstone with intercalations of marl and clay, as well as some limestone banks, reflecting a diverse depositional environment from fluvial to shallow marine. The secondary formations, pertaining to the Lower Cretaceous, specifically the Albien (Touahri et al., 2022; Kebili et al., 2021), are characterized by layers of clayey sandstone and clayey sand, overlaid by Quaternary-age dune belts.

According to hydrogeology, the area is influenced by the transboundary North Western Sahara Aquifer System (NWSAS), which is shared with Algeria, Tunisia, and Libya. This emphasizes the significance of transboundary water resources in this arid zone (Bouselsal, 2017; Satouh et al., 2021; Bouselsal et al., 2015). The study area is located at the southern limit of the NWSAS, where the Continental Intercalary (CI) aquifer outcrops. Composed mainly of sand, gravel, and sandstone formations, with variable proportions of clay dating from the Albien, this aquifer exhibits favorable porosity and permeability for the storage and movement of groundwater

under desert conditions. The thickness of the CI aquifer in Adrar does not exceed 250 meters. Piezometric map analysis indicates that the CI aquifer flows from northeast to southwest, a flow directed by the underlying topography and geology.

The potable water supply system in the study area utilizes wells tapping into the CI aquifer. Water is pumped from deep wells, with depths ranging from 200 to 250 meters, and each well has a flow rate varying from 20 to 50 liters per second. The pumped water is then collected in water towers. After chlorination, it is directly distributed, without any additional treatment, through the potable water supply network, which covers the various zones of the study region. The volume of water extracted from the Continental Intercalaire (CI) is approximately 250 million cubic meters per year (Benhamida, 2020).

3. Materials and methods

3.1. Sample collection and laboratory analysis

Sampling in the field and analysis in the lab of groundwater were performed across the study site, drawing samples from 25 wells that tap into the CI aquifer in Adrar. The locations for sampling are shown in Figure 2. The water samples were collected between May 8 and May 10, 2023, after 10 minutes of pumping to eliminate stagnant groundwater. The temperature of the water at the time of sampling ranged between 22 and 26 °C. To maintain a uniform methodology, the process for collecting and analyzing these groundwater samples was based on guidelines from the American Public Health Association (APHA, 2005). During the sampling expedition, the geographical coordinates for each site were documented using a Garmin e-Trex GPS unit. For each site, two 500 ml plastic bottles were used: one for cation analysis and the other for anion analysis. Cation samples were treated with high-grade HNO_3 to lower the pH to 2 directly at the sampling site. Immediately after collection, vital indicators like pH, Electrical Conductivity (EC), Total Dissolved Solids (TDS), and Temperature were recorded using a Hanna Multiparameter Waterproof Meter. All collected water samples were stored in a cooler at a temperature below 4°C and transferred to the ANRH laboratory in Adrar. There, they were kept in a refrigerator at a temperature below 4°C until analyzed, within a maximum period of three days. Key cations such as Na^+, Ca^{2+}, and K^+ were measured with a flame photometer, and Mg^{2+} concentration was determined using an inductively coupled plasma mass spectrometer (ICPMS). The level of chloride ions (Cl^-) was assessed through argentometric titration, while carbonate (CO_3^{2-}) and bicarbonate (HCO_3^-) levels were evaluated by titration with H_2SO_4. Furthermore, the concentrations of sulfate (SO_4^{2-}) and nitrate (NO_3^-)

were ascertained with a UV Spectrophotometer. Also, ion balance calculation was applied to the results of each analysis to assess the accuracy and dependability of the conducted analyses. The ionic balance is expressed as a percentage and is based on Equation (1).

$$\text{Ionic balance} = [(\Sigma \text{ cations} - \Sigma \text{ anions}) / (\Sigma \text{ cations} + \Sigma \text{ anions})] \times 100 \quad \text{(Eq. 1)}$$

Results were deemed acceptable in quality if the percentage error is below 5%.

3.2. Hydrochemistry of groundwater

Evaluating whether groundwater is potable requires comparing it to the recommended thresholds set by the World Health Organization (WHO, 2017). Thus, the concentration of each qualitative parameter in the water samples is assessed based on these standards to identify contaminated sources. Hydrochemical diagrams, such as those by Schoeller (1965) and Piper (1944) are used to determine hydrochemical facies and decipher the hydrochemical characteristics. They help categorize groundwater according to its chemical composition, highlighting the chemical diversity within an aquifer. These diagrams consider various factors, such as the flow model, water residence time, lithology, climate, and the dynamics of chemical reactions within the aquifer, thereby facilitating the comparative analysis of multiple samples on the same graph and allowing for the grouping of similar samples.

3.3. Multivariate statistical analysis

In order to shed light on hydrochemical processes, this work uses three well-known multivariate statistical techniques: principle component analysis (PCA), hierarchical cluster analysis (HCA), and multiple correlation analysis (MCA). The program XLSTAT was used to implement these techniques.

In this analysis, Pearson's correlation coefficient was employed to explore relationships within the dataset. Correlation levels were categorized based on their coefficient values (r). The interpretation of the correlation matrix focused on identifying statistically significant correlations (Mudgal et al., 2009; Hammad et al., 2023).

Principal Component Analysis (PCA) was extensively utilized in this study. PCA, a widely recognized technique in multivariate statistics, is known for its applicability across various scientific disciplines (Kharroubi et al., 2024; Farhat et al., 2019; Mahanty et al., 2023). It focuses on analyzing interrelated dependent variables, representing observed data matrices. In this research, PCA aimed to identify factors influencing water chemistry by interpreting chemical loadings on principal components.

On the other hand, Hierarchical Cluster Analysis (HCA) is commonly employed in water quality research. HCA provides a systematic approach to organizing large datasets into clusters, grouping them based on shared characteristics. Euclidean distances were used to measure dissimilarities between observation groups. This method aids in organizing data into distinct yet interconnected clusters, revealing underlying patterns in water quality studies.

3.4. Water pollution evaluation

3.4.1. The pollution index of groundwater (PIG)

The pollution index groundwater (PIG) technique was used to analyze the quality of the water in five steps (Verma and Singh, 2021; Subba Rao and Chaudhary, 2019; Kharroubi et al., 2024). First, each variable is given the appropriate relative weight (Rw) on a scale of 1 to 5, according to how much of an impact it has on the quality of drinking water (Table 1). The weighting coefficient (Wp), or the ratio of each element's Rw to the total of (RW) Eq.2, must be determined in the second phase.

$$\mathrm{WP} = \frac{\mathrm{RW}}{\sum(\mathrm{RW})} \qquad \text{(Eq. 2)}$$

The concentration (Ci) of each ion examined in the water samples was divided by the Drinking Water Quality Standards (DWHO) Eq. 3 (WHO, 2017) to estimate the (SOC) value in the following step.

$$\mathrm{SOC} = \frac{\mathrm{C_i^n}}{\mathrm{DWHO}} \qquad \text{(Eq. 3)}$$

To find the overall groundwater quality (OQG), multiply WP by SOC (Eq. 4) in the fourth step. At last, the PIG evaluation is completed by adding up all of the OQG values for every sample (Eq. 5).

$$\mathrm{OQG} = \mathrm{Wp} \times \mathrm{SOC} \qquad \text{(Eq. 4)}$$

$$\mathrm{PIG} = \sum \mathrm{OQG} \qquad \text{(Eq. 5)}$$

Water quality was categorized using PIG values, which were divided into five groups: low pollution (PIG: 1-1.5), moderate pollution (PIG: 1.5-2), high pollution (PIG: 2-2.5), and extremely high pollution (PIG > 2.5). Insignificant pollution was defined as PIG < 1.

Table 1. The parameters utilized in the computation of PIG.

Variable	(Rw)	(Rw)	DWHO
pH	5	0.1315	7.5
TDS (mg/l)	5	0.1315	500
TH mg/l ($CaCO_3$)	2	0.0526	300
Ca^{2+} (mg/l)	2	0.0526	75
Mg^{2+} (mg/l)	2	0.0526	30
Na^{+} (mg/l)	4	0.1052	200
K^{+} (mg/l)	1	0.0263	12
HCO_3^{-} (mg/l)	3	0.0789	300
Cl^{-} (mg/l)	4	0.1052	250
SO_4^{2-} (mg/l)	5	0.1315	200
NO_3^{-} (mg/l)	5	0.1315	50
	$\sum$ Rw=38	$\sum$ Rw=1	

3.4.2. Nitrate pollution assessment

Groundwater nitrate contamination may be measured using the Nitrate contamination Index (NPI) (Panneerselvam et al., 2022; Bahrami et al., 2022; Kharroubi et al., 2024). Equation 6 is used to generate this index. It takes into account HAV, the acceptable nitrate value, which is 20 mg/L, and Cs, the observed nitrate level in the water sample. The NPI categorizes pollution into five distinct levels: 'clean water' is indicated by a score of zero, reflecting no pollution; 'moderate pollution' corresponds to scores ranging from 1 to 2, indicating mild contaminants that may not pose immediate health risks; 'high pollution' is noted for scores from 2 to 3, suggesting significant contamination that can affect health; and 'extremely high pollution', which scores 3 or above, denotes severe contamination with substances particularly hazardous to drinking water quality. Awareness the water quality in the study region requires an awareness of this methodical methodology, which is fundamental to evaluating nitrate pollution.

$$\mathrm{NPI} = \frac{C_S - \mathrm{HAV}}{\mathrm{HAV}} \qquad \text{(Eq. 6)}$$

3.5. Health risk assessment

The health of people may be harmed by consuming water that contains excessive amounts of nitrates. Nitrate concentrations in the groundwater of the CI aquifer were compared to allowable limits while accounting for the age and sex of the subjects in order to determine the degree of non-carcinogenic danger (Egbueri et al., 2023; Kharroubi et al., 2024). The Health Risk Assessment method was created by the US Environmental Protection Agency (USEPA, 2001)

to evaluate and measure detrimental impacts on human health. A large number of scientists worldwide have used formulae (Eq. 7) to calculate the chronic daily intake (CDI (mg/kg/day)) in order to evaluate health hazards (Kharroubi et al. 2024; Houari et al. 2024). Table 1 offers a thorough summary of the information.

$$\mathrm{CDI} = \frac{\mathrm{C}\times\mathrm{IR}\times\mathrm{ED}\times\mathrm{EF}}{\mathrm{BW}\times\mathrm{AT}} \quad \text{(Eq. 7)}$$

In this formula, IR stands for ingestion rate, and C is the element/contaminant concentration (mg/l). It is 3 liters per day for adults (women and men), 1.5 liters per day for children, and 0.7 liters per day for infants, according to field surveys and studies based on climatic conditions; EF stands for exposure frequency (days/year), which is approximately 365 days per year for adults, children, and infants; ED is the number of years that the individual is exposed to the contaminant (adults: 30 years; children: 16 years; infants: 1 year); BW is the average body weight (adults: 57.5 kg; children: 18.7 kg; infants: 6.9 kg) (USEPA 1989); AT represents the average exposure duration in days. It is calculated by multiplying the number of years during which an individual is exposed to the contaminant (ED) by the number of days per year, which is 365 days.

A hazard quotient (HQ) may be used to show that a pollutant has no cancer-causing properties (Egbueri et al. 2023; Shaikh et al. 2020). Equation 8 may be used to compute the HQ:

$$\mathrm{HQ} = \frac{\mathrm{CDI}}{\mathrm{RfD}} \quad \text{(Eq. 8)}$$

The reference dose (RfD) for the contaminant is 1.6 mg/(kg day) for nitrate, (Adimalla and Qian, 2019; Adimalla, 2020b). An HQ >1 indicates an unacceptable level of the pollutant in drinking water, and HQ <1 indicates a safer level for human health (Kharroubi et al., 2024; Kaur et al., 2020; Dhakate et al., 2023).

4. Results and discussion

4.1 Physico-chemical parameters and assessment of potability

In this study, a comprehensive analysis of 12 water quality parameters was conducted on all groundwater samples. Table 2 presents a detailed summary of these parameters, including their range of minimum to maximum values, mean values, instances of exceeding limits, and reference standards for drinking water according to the World Health Organization guidelines (WHO, 2017).

Data on the quality of groundwater in the Continental Intercalary (CI) of Adrar show that the pH range of the CI groundwater was 7.15 to 8.07. The large range of electrical conductivity (EC) values (1150 to 3360 µS/cm) in CI waters indicates considerable mineralization. Water

that has a conductivity of more than 1500 µS/cm is deemed inappropriate (WHO, 2017). 68% of CI groundwater samples are considered unsuitable for direct human consumption without previous treatment, as per the 2017 WHO recommendations. The samples' total dissolved solids (TDS) ranged from 713 to 2229 mg/L, with an average of 1225 mg/L. Of the samples examined, 68% had TDS levels over the WHO-recommended threshold. Kidney stones, digestive problems, and cardiovascular disorders may result from prolonged exposure to elevated TDS levels (Sahu et al., 2018; Subba Rao et al., 2019).

The total concentration of magnesium and calcium ions in water, which is irreversible upon boiling, is called total hardness (TH). In groundwater samples, the measured total hardness (TH) value varied from 266 to 607 mg/L, with an average of 439 mg/L. Sixty-eight percent of the water samples are below the 500 mg/L allowable consumption level; the remaining samples are beyond this limit. It is observed that a value of TH > 300 mg/L indicates very hard water, whereas a value between 150 and 300 mg/L indicates hard water. 96% of the samples are categorized as extremely hard, while just 4% are classed as hard. Frequent ingestion of water with a high concentration of TH may induce renal stones and cardiovascular issues in people. Higher levels of hardness exposure will also make eczema worse. A high TH content causes scale deposits in pipes and boilers, an alkaline taste in drinking water, and poor soap and detergent effectiveness.

When TDS and TH were plotted bivariately (Fig. 4), it was shown that 32% of the samples were freshwater (TDS <1000 mg/l) and 68% were brackish (Freeze and Cherry, 1979), with hardness varying from mild to very hard (Sawyer and McCarty, 1978; Arfa et al., 2022). Groundwater samples show a shift from fresh to brackish conditions based on TDS.

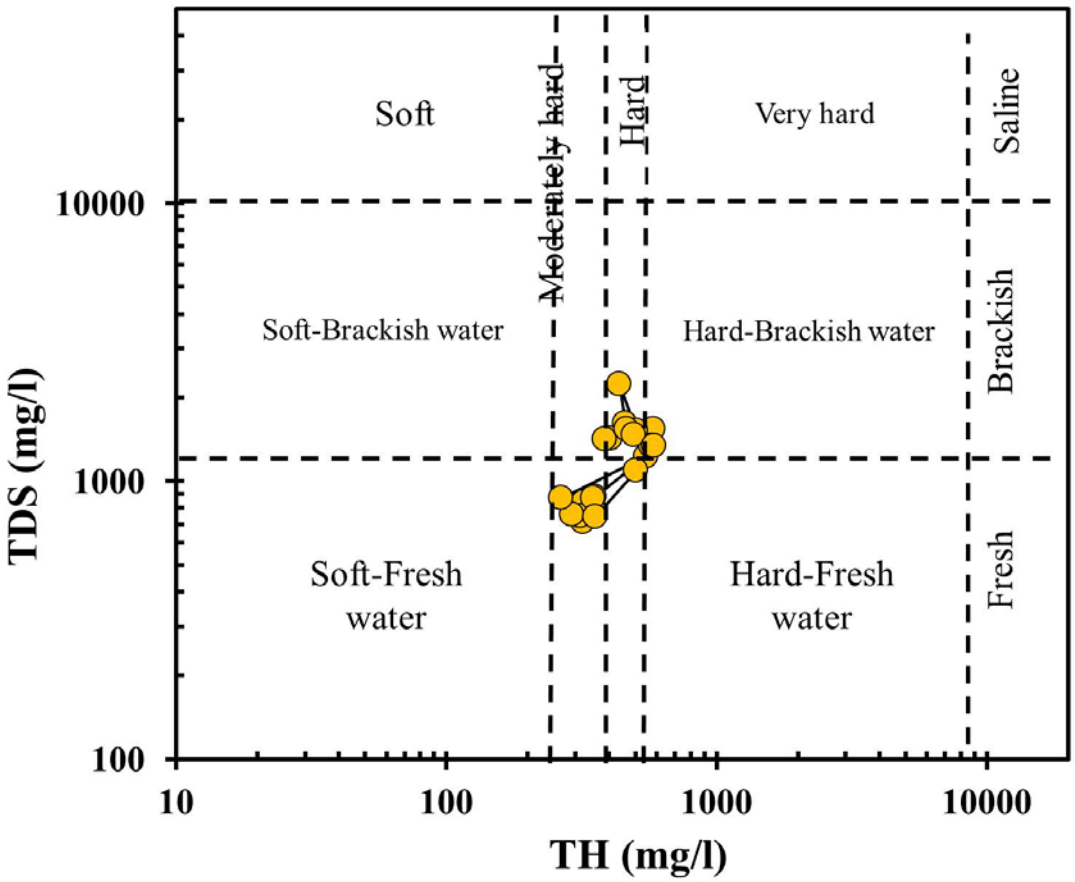

Figure 4. Binary diagram of TH vs. TDS.

High levels of calcium can cause gastric problems, while a deficiency in Ca^{2+} in drinking water can contribute to the formation of kidney stones, strokes, hypertension, and colorectal cancer (Sengupta, 2013). The average calcium content in CI waters is 75.59 mg/l, with a range of 34 to 126 mg/l. The average sodium content in CI waters is 223.19 mg/l, varying from 110 to 500 mg/l, with all samples recording levels below the permissible limit. High levels of sodium pose a risk of cardiovascular and circulatory problems (Haritash et al., 2008). The potassium levels in all the samples were above the advised threshold of 12 mg/l, with the exception of the borehole labeled CI-08. The observed range of potassium variation was between 12 and 40 mg/l. Such concentrations may pose risks of neurological and gastrointestinal problems (Ramesh and Soorya, 2012).

High amounts of chloride can lead to high blood pressure, with chloride ion content in CI water ranging from 161 to 798 mg/l, averaging 342.07 mg/l, and only one sample (CI-17) exceeding the 600 mg/l limit. The dietary significance of chlorine is notable in the release of sodium chloride (NaCl), especially in chronic cardiac conditions (WHO, 2017). The sulfate concentration in CI water varies from 172 to 472 mg/l, with an average of 300.96 mg/l. Only

20% of the samples were above the WHO-established permissible limit of 400 mg/l. High levels of sulfate can lead to laxative effects, a bitter taste, and health complications such as dehydration, diarrhea, and abdominal pain (Karunanidhi et al., 2021).

Bicarbonate is formed during the decomposition of soil organic matter, involving root respiration and humus degradation, producing CO_2, which reacts with rainwater to form bicarbonate ions. In water, bicarbonate primarily affects pH and can cause deposits in pipes. Generally, it does not pose a major health risk, but high levels can impact water quality and appliances. In the studied area, bicarbonate levels in groundwater ranged from 52 to 181 mg/l, with an average of 151.20 mg/l. All samples were below the WHO-recommended safe level.

High levels of nitrate in groundwater are mainly due to excess agricultural fertilizers, waste from animals and humans, and plant debris. In drinking water, the maximum allowable concentration of nitrate is 50 mg/l. However, in the studied area, nitrate concentrations range from 8 to 58 mg/l, with 20% of the samples exceeding the limit recommended by the World Health Organization in 2017 (Arfa et al., 2022).

Table 2. Data on the parameters affecting groundwater quality in the studied area.

Variable	Units	Minimum	Maximum	Average	Standard deviation
Ca^{2+}	mg/l	34	126	75,59	25,13
Mg^{2+}	mg/l	30	95	59,93	16,14
Na^{+}	mg/l	110	500	223,19	92,53
K^{+}	mg/l	12	40	21,14	6,54
Cl^{-}	mg/l	161	798	342,07	152,13
SO_4^{2-}	mg/l	172	472	300,96	89,03
HCO_3^{-}	mg/l	52	181	151,20	27,05
NO_3^{-}	mg/l	9	58	34,67	14,52
pH	/	7,15	8,07	7,77	0,25
TDS	mg/l	713	2229	1225,52	364,76
EC	µS/cm	1150	3360	1971,60	566,62
TH	mg/l ($CaCO_3$)	266	607	439	104,52

4.2. Groundwater hydrochemistry

4.2.1. Hydrochemical facies

Schoeller (1965) developed a semi-logarithmic diagram to represent the concentrations of major ions in water, expressed in meq/l. In this diagram (Fig.5), the concentration levels of each ion for each water sample are indicated by points located on evenly spaced lines. These points are then connected by dashed lines, thus illustrating the absolute concentration of each ion as well as concentration variations among different groundwater samples. Additionally, the diagram allows for determining the ratio between two specific ions within the same sample. Figure 2 illustrates the application of the Schoeller diagram to demonstrate the ionic composition of groundwater in the study area. The analyzed water samples are represented by colored lines, highlighting the order of ion concentrations as follows: $Na^+ > Ca^{2+} > Mg^{2+} > K^+$ and $Cl^- > SO_4^{2-} > HCO_3^- > NO_3^-$, except for wells CI-07, CI-08, and CI-23, which show a sodium sulfate facies. The near parallelism of the lines suggests a common origin of CI water, primarily characterized by evaporitic sources (gypsum and halite), with high concentrations of Na^+ and Cl^-, as well as Ca^{2+} and SO_4^{2-}. The mere variation in water chemical composition is attributed to lithological changes in the reservoir and anthropogenic influences. These observations corroborate the conclusions drawn in the previous chapter.

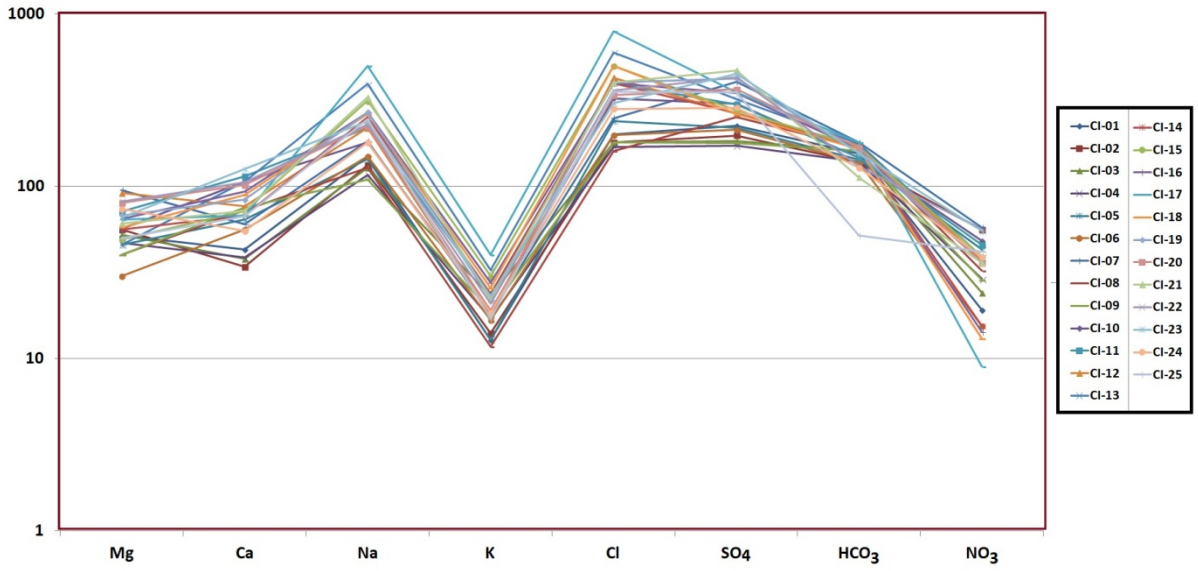

Figure 5. Schoeller's diagram illustrates the variation in concertations of chemical elements in CI waters.

The Piper diagram, developed by Piper in 1944 and based on an earlier model by Hill in 1940, is a graphical tool that illustrates the chemical equilibrium of cations and anions in water. This

diagram includes three parts: (i) the lower left section, which represents cations (Mg, Ca, and Na+K), (ii) the lower right section for anions (Cl, SO_4, and HCO_3), and (iii) a central diamond-shaped graph that combines the data from the two ternary diagrams. This tool is crucial for the visual analysis of numerous groundwater samples. In the Piper diagram shown in Figure 6, groundwater samples from the studied area are classified into two categories. The first category, Ca–Mg–SO_4–Cl, accounts for 60% of the samples and is located in the northeast part of the area, upstream of the aquifer, with relatively low electrical conductivity (EC < 1900 µS/cm). The second category, Na–Cl, includes 40% of the samples located downstream, in the south and southwest regions, characterized by high conductivity (EC > 1900 µS/cm). The presence of these different water types indicates the complexity of mineralization processes occurring in the region.

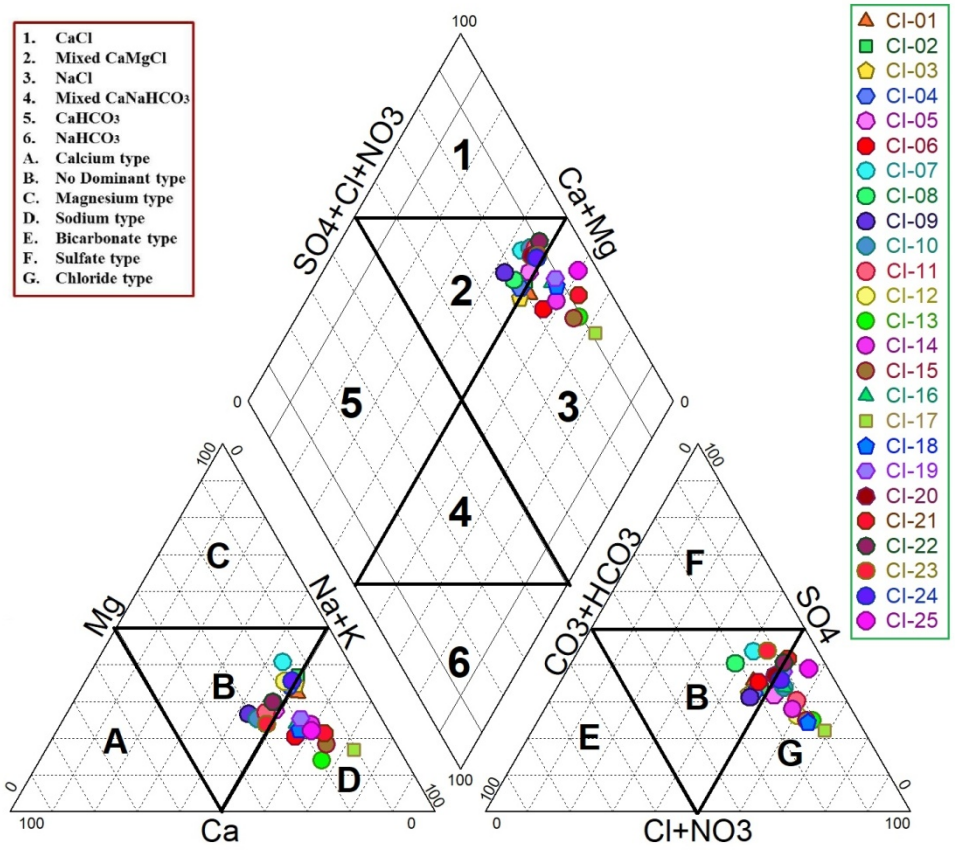

Figure 6. Piper diagram of Adrar CI waters.

4.2.2. Origin of nitrates in CI groundwater

Human activity has a significant impact on the chemistry of groundwater. Indeed, the chemical composition is altered by the infiltration of municipal wastewater beneath urban centers and agricultural drainage water beneath cultivated lands. In the studied area, the main contaminant affecting groundwater quality is nitrate. The measured concentrations of NO_3^- vary between 9 and 58 mg/l, with an average of 39 mg/l, thus exceeding the acceptable limit of 50 mg/L set by the WHO in 2017 for 24% of the analyzed samples. In natural water, unaffected by human intervention, the concentration of NO_3^- generally does not exceed 20 mg/l (Spalding and Exner, 1993; Egbueri et al., 2023). Any value above this limit indicates anthropogenic contamination. Due to its high solubility and significant mobility, nitrate present in groundwater is a useful tool for determining the intensity of human activity (Egbueri, 2023; Bouselsal and Saibi, 2022). The main sources of NO_3^- in these waters are related to domestic wastewater discharge and agricultural practices, explaining the high concentrations observed. An in-depth analysis was conducted to examine the mechanisms regulating the hydrogeochemistry of nitrate-enriched groundwater.

The Cl^-/Na^+ molar ratios compared to NO_3^-/Na^+ graph is a widely recognized tool for assessing nitrate sources in groundwater (Zhang et al., 2023). As shown in Figure 7a, the observed Cl^-/Na^+ and NO_3^-/Na^+ ratios in groundwater samples range from 0.78 to 1.26 and from 0.15 to 0.01, with average values of 0.98 and 0.06 respectively. These ratios provide insight into the relative abundance of chloride, nitrate, and sodium ions in groundwater. The stoichiometric processes governing the relationships between these ions are essential for understanding nitrate sources. For example, the presence of high Cl^-/Na+ ratios indicates potential contamination from sources rich in chloride ions, such as wastewater or industrial effluents. Meanwhile, NO_3^-/Na^+ ratios highlight the contribution of NO_3^-, with higher values suggesting inputs of nitrate from agricultural fertilizers or organic waste (Agbasi et al., 2023). Additionally, the position of the samples on the graph suggests that agricultural activities and domestic discharge are the main contributors to water pollution in the region. This inference aligns with the observed Cl^-/Na^+ and NO_3^-/Na^+ ratios, indicating potential contamination from agricultural runoff and domestic wastewater discharge, both of which are known sources of nitrate pollution in groundwater (Zhang et al., 2023; Amiri et al., 2022).

To exclude the impact of groundwater salinity or dilution on the identification of nitrate sources, the NO_3^-/Cl^- ratio was applied (Zhang et al., 2023; Amiri et al., 2022). Generally, highly saline

waters have a low NO_3^-/Cl^- ratio under natural conditions, indicating anthropogenic influence such as inputs from agricultural, domestic, and municipal pollutants (Luo et al., 2018). The sampled groundwater is predominantly associated with residential inputs, as illustrated in Figure 7b. This indicates that domestic wastewater accounts for the majority of nitrates present in groundwater, with very little originating from agricultural practices. In other words, nitrate-enriched groundwater in the study region is predominantly found in residential areas as opposed to agricultural zones, confirming that groundwater hydrochemistry is heavily influenced by domestic effluents from residential areas.

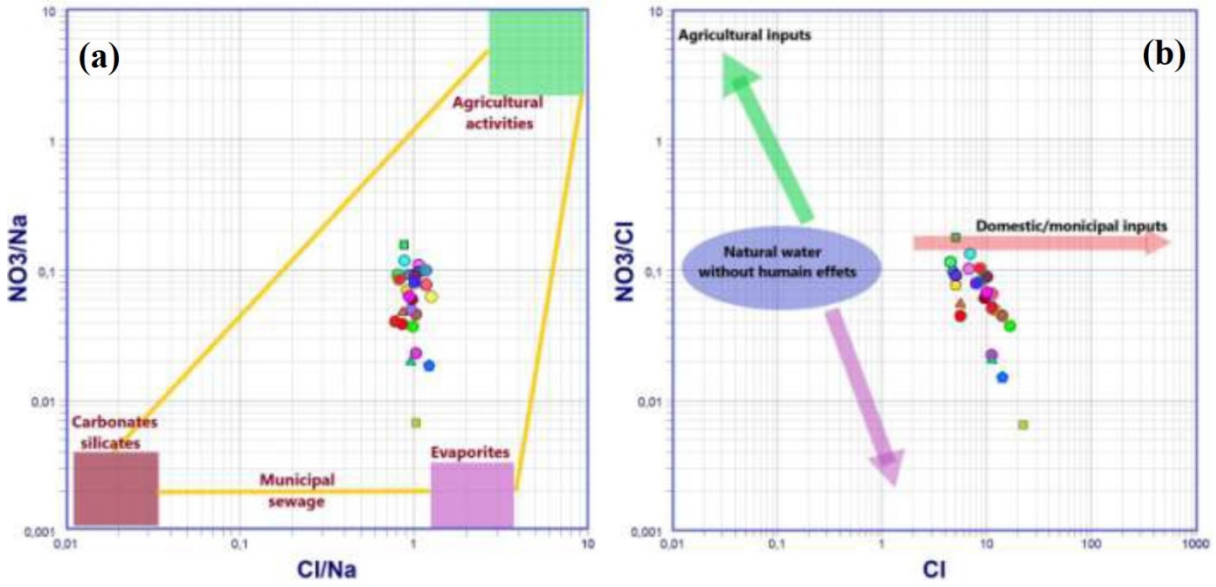

Figure 7. Binary diagram of: (a) Cl^-/Na^+ vs. NO_3^-/Na^+ (b) Cl^- vs. NO_3^-/ Cl^-.

4.3. Multivariate analyses

4.3.1. Correlation matrix

The correlation matrix allows for the detection of existing relationships between different variables, whether positive or negative. It aggregates correlations between multiple variables and extracts coefficients indicating the influence of variables on each other. Examination of Table 4, regarding the correlation matrix, reveals that some parameters are consistently correlated with each other across all analyses, while others are correlated in one analysis but not in another. Most correlations between groundwater parameters are positive. There is a strong correlation between electrical conductivity on one hand, and chlorides, sodium, calcium, sulfates, and potassium on the other hand. Similar correlations are observed between these parameters and TDS. In both cases, the correlation is positive and allows for deducing the major

elements responsible for the increase in mineralization and salinity of the studied waters (Bouselsal and Belksier, 2018; Bouselsal and Saibi, 2022; Hao et al., 2022).

Other significant correlations are found between potassium and chlorides, sodium and chlorides, sulfates and calcium, sulfates and magnesium. These relationships illustrate the complexity of the geochemical mechanisms governing the mineralization of groundwater in the Continental Intercalary aquifers of the studied area, particularly the dissolution of sulfates and halite. Negative correlations between nitrate (NO_3^-) on one hand, and other parameters on the other hand, indicate the anthropogenic origin of this element in the CI waters.

Table 3. Correlation matrices of hydrochemical parameters of CI waters.

Variables	**Ca^{2+}**	**Mg^{2+}**	**Na^+**	**K^+**	**Cl^-**	**SO_4^{2-}**	**HCO_3^-**	**NO_3^-**	**pH**	**TDS**	**EC**
Ca^{2+}	**1**										
Mg^{2+}	0,29	**1**									
Na^+	0,37	0,18	**1**								
K^+	0,35	0,09	0,86	**1**							
Cl^-	0,41	0,23	**0,95**	**0,87**	**1**						
SO_4^{2-}	**0,59**	**0,56**	**0,56**	0,31	0,43	**1**					
HCO_3^-	0,14	0,18	0,16	0,36	0,24	-0,12	**1**				
NO_3^-	0,27	0,39	-0,20	-0,32	-0,24	0,35	-0,24	**1**			
pH	-0,01	-0,15	0,31	0,34	0,29	0,03	-0,04	-0,05	**1**		
TDS	**0,54**	0,42	**0,92**	**0,82**	**0,93**	**0,63**	0,26	-0,17	0,22	**1**	
EC	**0,57**	0,43	**0,91**	**0,81**	**0,92**	**0,65**	0,26	-0,15	0,22	0,99	**1**

4.3.2. Principal Component Analysis

The Principal Component Analysis (PCA) conducted on the groundwater data from Adrar's Continental Intercalary (CI), encompassing 11 parameters across 25 samples, revealed a critical understanding of the geochemical processes shaping their composition. The results indicate that the first two principal components, collectively representing 69.37% of the total variance (Fig.8), effectively encapsulate significant variations within the dataset. Specifically, the first extracted principal component (PC1) explains 50.59% of the total variance and is characterized by high loadings of TDS, EC, Cl^-, K^+, and Na^+, as well as moderate loadings of SO_4^{2-}, Mg^{2+}, Ca^{2+}, and HCO_3^-. PC1 signifies salinization, encompassing natural processes such as the

dissolution of evaporites (halite and/or gypsum) and non-conservative transport phenomena (such as ion exchange with clay minerals).

However, the second component (PC2), which accounts for 18.78% of the variation overall, is mostly impacted by NO_3^-. This implies that anthropogenic inputs have a role in groundwater mineralization, demonstrating how human activity affects groundwater quality (Kharroubi et al., 2024; Amiri et al., 2022; Kebili et al., 2021; Bouselsal, 2016).

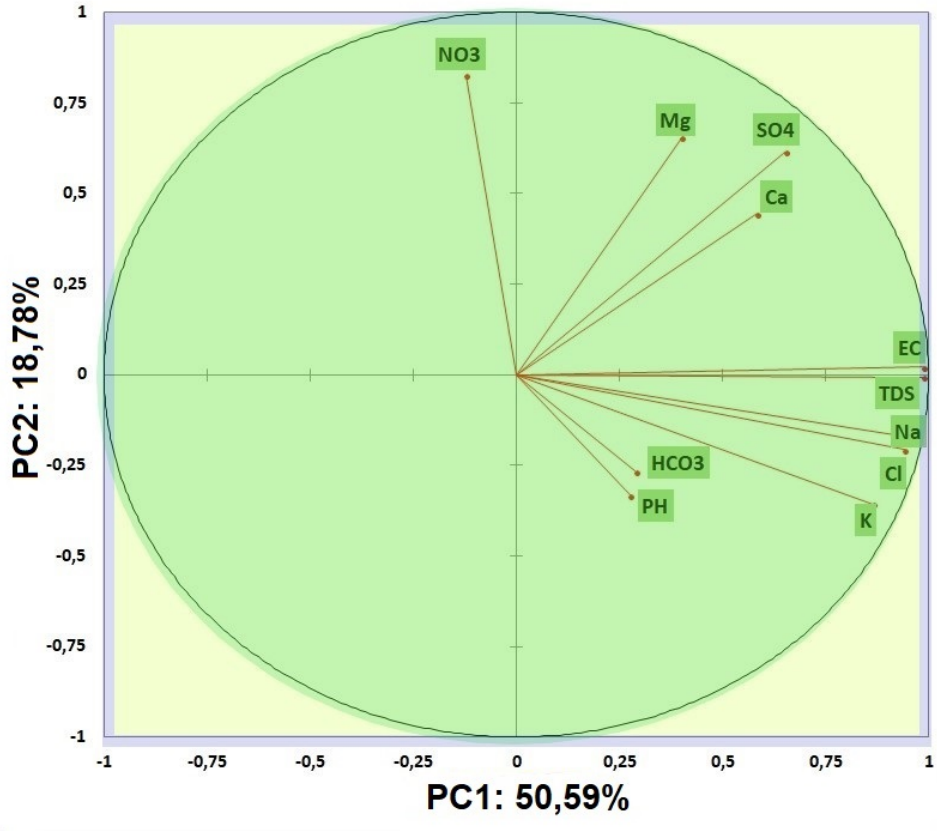

Figure 8. Analysis of principal components of CI waters.

4.3.3. Hierarchical clustering analysis

The hierarchical clustering analysis (HCA) technique is widely used to categorize water samples in many surveys and is based on a comprehensive analysis of multiple parameters, resulting in the grouping of samples based on their mutual similarities (Egbueri, 2019; Kharroubi et al., 2024; Ouarekh et al., 2022). The dendrogram produced by this approach, which utilizes Euclidean distance, reveals distinct clusters. Within each group, the samples exhibit greater similarity to each other than to samples from different groups. In the context of this research, hierarchical cluster analysis (HCA) identified three main clusters (Fig. 9):

Group 1: Comprising samples with electrical conductivity below 1400 µS/cm, this group is located in the northeastern part of the region, upstream of the aquifer, an area less affected by urbanization and agricultural activities.

Group 2: Samples in this group, characterized by electrical conductivity ranging from 1400 to 2360 µS/cm, mainly come from agricultural areas in the northeastern part of the study region and north of the city of Adrar. These groundwater sources are influenced by the infiltration of irrigation water laden with chemical fertilizers and wastewater under urban areas.

Group 3: This cluster includes samples displaying electrical conductivity exceeding 2280 µS/cm, predominantly situated downstream of the aquifer, in the southern part of the analyzed area. The origin of this high electrical conductivity can be attributed to the accumulation of dissolved ions as they move through geological strata containing soluble salts, human pollution due to infiltration of wastewater under urban areas, and the penetration of irrigation water enriched with chemical fertilizers and soluble salts, as a consequence of evaporation in a semi-arid environment.

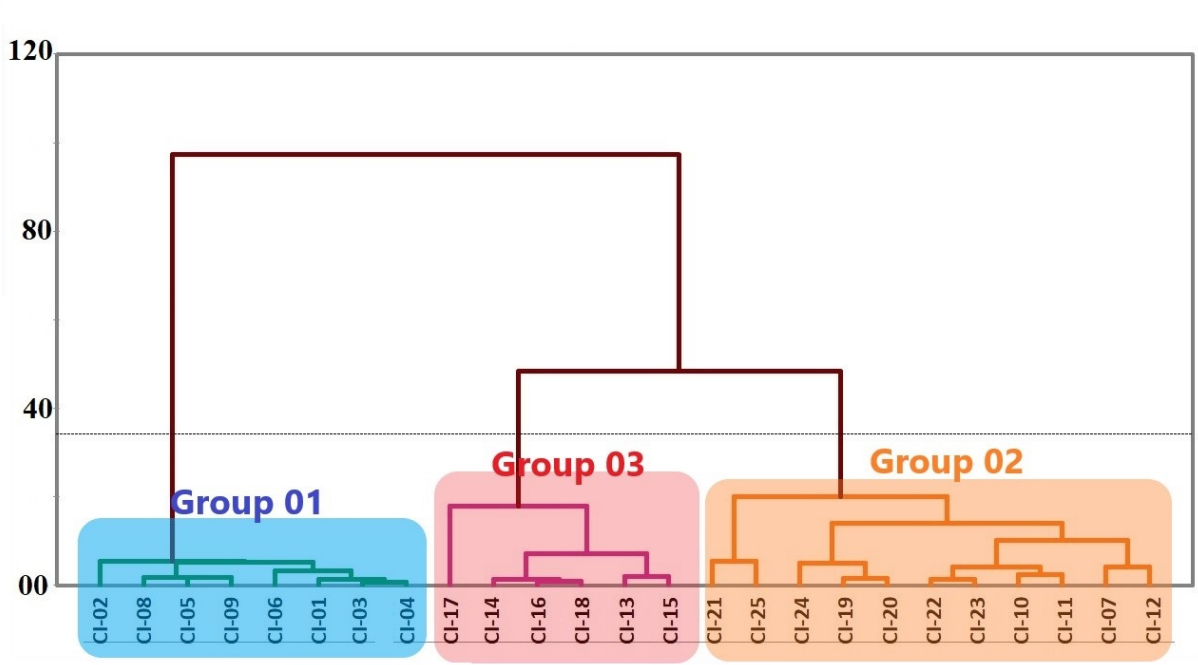

Figure 9. Hierarchical cluster analysis of CI waters.

4.5. Groundwater pollution and risk assessment

4.5.1. The pollution index of groundwater (PIG)

The PIG method was first described by Subba Rao in 2012. This method is based on the integration of various physico-chemical characteristics. It combines all parameters related to water quality into a unified indicator, as previously discussed by researchers (Egbueri, 2019; Subba Rao and Chaudhary, 2019). Furthermore, the PIG framework has enabled a comparative analysis of water quality across different samples and facilitated the monitoring of its temporal variations. In the studied region, the average PIG is 1.29, with a range from 0.87 to 1.90. The results show that 28%, 48%, and 24% of the CI water samples are classified as having insignificant, low, and high pollution, respectively (Table 4). This indicates that the Continental Intercalaire aquifer is experiencing increasing contamination due to anthropogenic surface phenomena such as urbanization and agricultural activity. The lowest values are found in the upstream part of the aquifer in wells CI-04 (0.87), CI-03 (0.90), and CI-06 (0.90), while the highest values are found in the downstream part of the aquifer at wells CI-17 (1.90) and CI-22 (1.55) (Fig. 10). This deterioration is influenced by the severe climatic conditions of the region, which contribute to the increase in groundwater salinity, as well as by human activities introducing pollutants such as nitrates.

Table 4. Parameter calculation results: NPI, PIG and HQ.

N° wells	NPI	PIG	HQ-Adult	HQ-child	HQ-infant
CI-01	-0,04	0,93	0,63	0,96	1,22
CI-02	1,80	0,97	1,83	2,81	3,55
CI-03	0,21	0,90	0,79	1,21	1,53
CI-04	0,45	0,87	0,95	1,45	1,84
CI-05	1,15	1,03	1,40	2,16	2,73
CI-06	-0,23	0,90	0,51	0,78	0,98
CI-07	1,88	1,42	1,88	2,89	3,66
CI-08	0,61	0,96	1,05	1,62	2,04
CI-09	0,43	0,90	0,93	1,43	1,81
CI-10	1,42	1,29	1,58	2,42	3,07
CI-11	1,29	1,51	1,50	2,30	2,91
CI-12	0,85	1,42	1,21	1,85	2,35
CI-13	0,95	1,65	1,27	1,96	2,47
CI-14	-0,23	1,31	0,51	0,78	0,98
CI-15	0,95	1,45	1,27	1,96	2,47

CI-16	-0,29	1,44	0,47	0,71	0,90
CI-17	-0,55	1,90	0,29	0,45	0,57
CI-18	-0,35	1,41	0,42	0,65	0,83
CI-19	0,83	1,50	1,19	1,83	2,31
CI-20	0,80	1,43	1,17	1,80	2,28
CI-21	0,80	1,52	1,17	1,80	2,28
CI-22	1,80	1,55	1,83	2,81	3,55
CI-23	1,75	1,53	1,79	2,76	3,49
CI-24	0,95	1,22	1,27	1,96	2,47
CI-25	1,10	1,27	1,37	2,11	2,66
Mean	0,73	1,29	1,13	1,74	2,20
Max	1,88	1,90	1,88	2,89	3,66
Min	-0,55	0,87	0,29	0,45	0,57

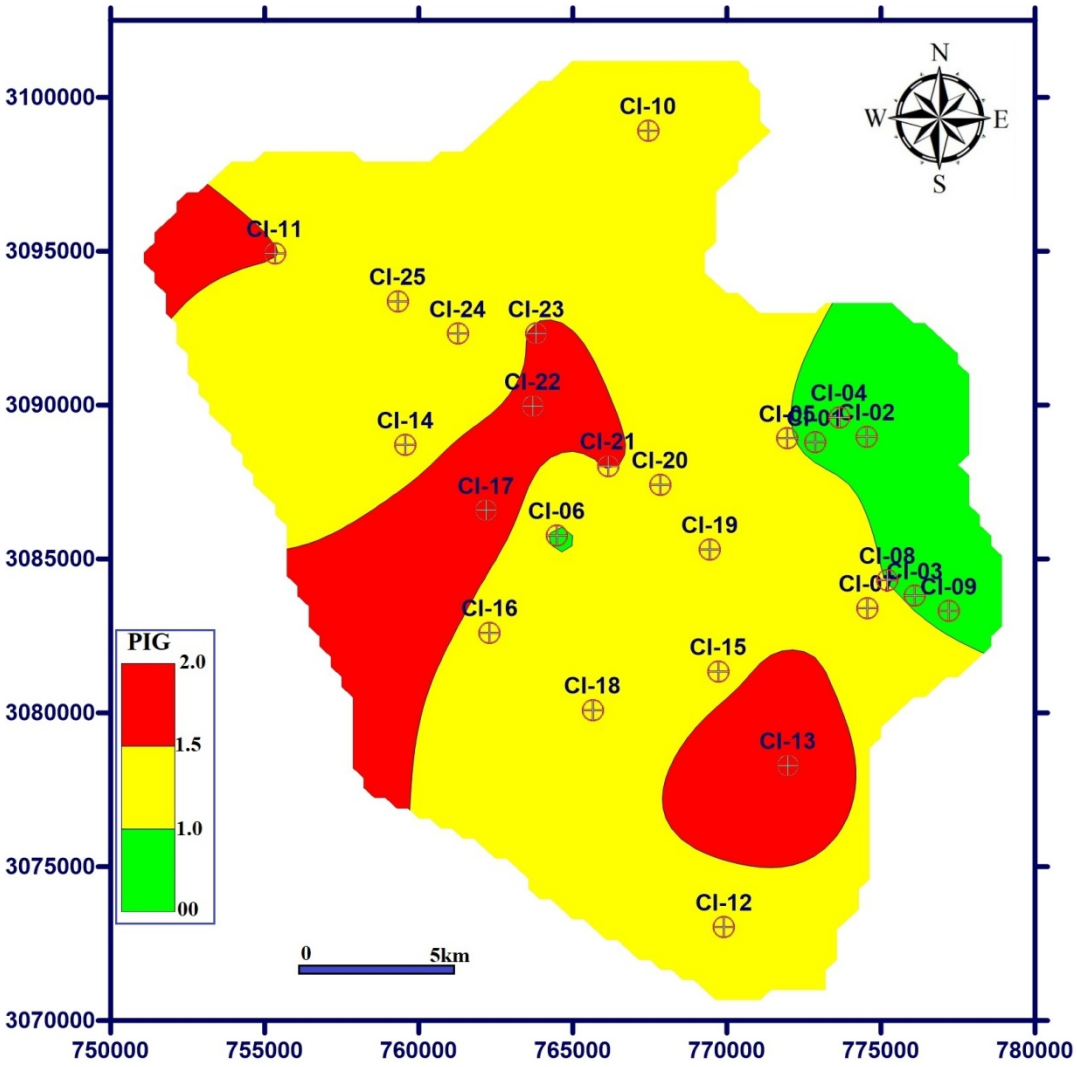

Figure 10. Spatial Distribution of the Groundwater Pollution Index (GPI) Values.

4.5.2. Nitrate Pollution Index (NPI)

Excessive levels of nitrates in groundwater and river water, the main sources of drinking water, can pose environmental, economic, social, and public health challenges. Nitrates (NO_3^-) in water can transform into nitrites (NO_2^-) in the human body through a simple chemical reduction process. Nitrites reduce the ability of hemoglobin to transport oxygen to cells, potentially leading to methemoglobinemia, or "blue baby syndrome" (Obeidat et al., 2012; Adimalla and Qian, 2019). Although this condition is rare and primarily observed in newborns after ingesting water rich in nitrates, the precautionary principle has led the World Health Organization to recommend a maximum limit of 50 mg/l of nitrates in drinking water.

The Nitrate Pollution Index (NPI) serves as an effective measure to assess the extent of nitrate contamination. The classification of NPI levels in groundwater in the study area is depicted in Figure 11a. In the study area, NPI values range from -0.55 to 1.88 (Table 4). Approximately

24% of the samples show insignificant pollution, while 44% exhibit slight pollution, and 32% are classified as having moderate pollution. The distribution map of NPI indicates that sites heavily polluted by nitrates are widespread south of Adrar Airport, north of Adrar City, and in the agricultural areas of the northwest of the study area. Conversely, the lowest values are found in the southern part of the study area.

4.5.3. Health risk assessment

In the studied area, 20% of the measured nitrate concentrations exceed the WHO standard set at 50 mg/l, indicating a high risk associated with the consumption of groundwater containing high levels of nitrates. Comparing this data with land use in the region, it is observed that the increase in nitrate levels corresponds to the density of urban fabric and agricultural areas. The shallow depth of the aquifer and the superficial geological formations mainly composed of sand facilitate the infiltration of water rich in nitrogen compounds into the aquifer due to the high solubility of nitrates. These nitrate-rich waters eventually get tapped by wells intended for drinking water supply.

Risk index values were assessed for infants, children, and adults (Table 4). The Hazard Quotient (HQ) value for infants ranged from 0.57 to 3.66 with an average value of 2.20, for children it ranged from 0.45 to 2.89 with an average of 1.74, and corresponding values for adults were from 0.29 to 1.88 with an average of 1.13. In the studied area, it was found that 80% of groundwater samples intended for infants, 76% of groundwater samples intended for children, and 64% of groundwater samples intended for adults had Hazard Quotient (HQ) values greater than 1, indicating a substantial risk for residents.

The spatial distribution of health risk indices highlights a significant concern for infants who, across much of the study area, are exposed to risks associated with the consumption of groundwater high in nitrates, exhibiting Hazard Quotient (HQ) values exceeding 1, with the notable exception of four wells located in the south, as illustrated in Figure 11b. Furthermore, it is observed that infants are subjected to severe health risks, with HQ values surpassing 3 in 16% of cases, a condition attributed to high nitrate concentrations resulting from dense population and intensive agricultural practices in the region.

The distribution of risk indices also reveals a concern for children, who face similar risks from consuming groundwater high in nitrates, with HQ values exceeding 1, except for six wells, five situated in the south and one in the northeast of the study area, as depicted in Figure 11c. This

exposure slightly varies from that of infants, suggesting a spatially specific risk distribution for each age group.

Regarding adults, the risk associated with consuming nitrate-rich groundwater is less pronounced compared to infants and children. This difference is primarily due to their larger body mass, making potential effects less severe. Nevertheless, a risk remains, especially in the southern part of the study area, as presented in Figure 11d.

The data thus suggest the need to adopt differentiated strategies to address health risks associated with nitrates in groundwater, taking into account the varying sensitivity among different age groups and the geographic distribution of these risks. These findings highlight the critical importance of health issues associated with the consumption of water contaminated with nitrates, emphasizing the imperative to act promptly. It is essential to implement water treatment infrastructure to purify it before integration into the drinking water distribution network, aiming to mitigate these dangers.

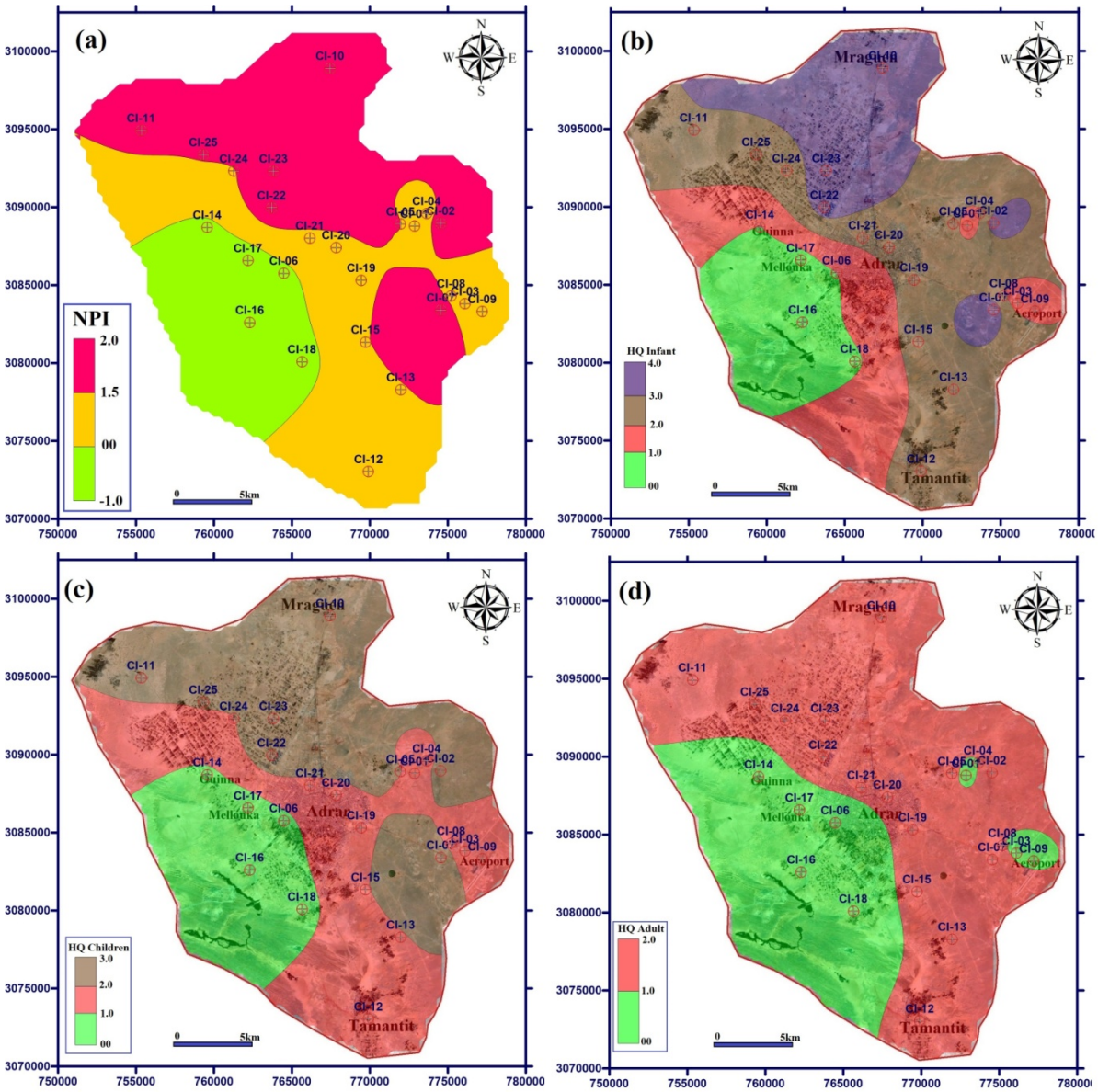

Figure 11. Spatial Distribution of: (a) Nitrate Pollution Index (NPI), and Hazard Quotient (HQ) for (b) Infants, (c) Children and (d) Adults in the Study Area.

5. Conclusion

This study was driven by two main objectives: to assess the potability and safety of water from the Continental Intercalary (CI) aquifer in the Adrar region for human consumption, and to quantify the health risks associated with nitrate contamination across different age groups within the local population. The study employed WHO guidelines, hydrochemical diagrams, multivariate statistical analyses, as well as the Pollution Index of Groundwater (PIG), Nitrate Pollution Index (NPI), and Health Risk Assessment (HRA), in accordance with USEPA methodology.

Hydrochemical analysis and multivariate statistical analysis revealed the influence of anthropogenic phenomena and processes of evaporation and dissolution of evaporites on groundwater mineralization. Consequently, 68% of the samples were classified as brackish, compromising their direct consumption and posing infrastructural risks.

The study identified elevated nitrate levels, ranging from 8 to 58 mg/L, with 20% of the samples exceeding the WHO limit of 50 mg/L, primarily due to agricultural and urban sources. The PIG delineated a spectrum of pollution levels ranging from insignificant (28%), low (48%), to high (24%). Meanwhile, the NPI indicated that 24% of the samples showed insignificant pollution, while 44% exhibited slight pollution and 32% moderate pollution.

The HRA demonstrated significant non-carcinogenic risks associated with nitrate exposure, with 80% of groundwater samples for infants, 76% for children, and 64% for adults showing hazard quotient (HQ) values exceeding 1. Alarmingly, 16% of the samples for infants had HQ values exceeding 3. Spatial analysis indicated that most infants in the study area are at high risk from nitrates, except for some safer wells in the south. Children also face considerable risks, with slight variations in risk distribution suggesting localized differences in nitrate exposure. Adults, though less affected, still face risks, particularly in the southern part.

Given the significant health risks associated with elevated nitrate levels, especially for vulnerable populations such as infants and children, this study underscores the urgent need to develop strategies addressing both the symptoms and sources of contamination. This includes improving agricultural practices, waste management, and implementing robust groundwater monitoring frameworks to ensure the safety and sustainability of water resources in the Adrar region.

References

Adimalla, N., Qian, H., 2019. Groundwater quality evaluation using water quality index (WQI) for drinking purposes and human health risk (HHR) assessment in an agricultural region of Nanganur, south India. Ecotoxicology and Environmental Safety 176: 153–161. https://doi.org/10.1016/j.ecoenv.2019.03.066

Adimalla, N., Ajay, K.T., 2020a. Hydrogeochemical Investigation of Groundwater Quality in the Hard Rock Terrain of South India Using Geographic Information System (GIS) and Groundwater Quality Index (GWQI) Techniques. Groundwater for Sustainable Development 10: 100288. https://doi.org/10.1016/j.gsd.2019.100288.

Adimalla, N., 2020b. Spatial distribution, exposure, and potential health risk assessment from nitrate in drinking water from semi-arid region of South India. Hum. Ecol. Risk Assess. 26 (2), 310–334. https://doi.org/10.1080/10807039.2018.1508329.

Agbasi, J.C., Egbueri, J.C., 2023. Intelligent soft computational models integrated for the prediction of potentially toxic elements and groundwater quality indicators: a case study. Journal of Sedimentary Environments 8(1): 57-79. https://doi.org/10.1007/s43217-023-00124-y

Amiri, V., Sohrabi, N., Li, P., Amiri, F., 2022. Groundwater Quality for Drinking and Non-Carcinogenic Risk of Nitrate in Urban and Rural Areas of Fereidan, Iran. Exposure and Health 15: 807–823. https://doi.org/10.1007/s12403-022-00525-w

American Public Health. (APHA), 2005. Standard methods for the examination of water and wastewater, 21st edn. American Public Health Association, Washington.

Bahrami, M., Zarei, A.R., Rostami, F., 2020. Temporal and spatial assessment of groundwater contamination with nitrate by nitrate pollution index NPI and GIS case study: Fasarud Plain, southern Iran. Environmental Geochemistry and Health 42: 3119–3130. https://doi.org/10.1007/s10653-020-00546-x

Benhamida, S.A., 2020. Approcche géochimique à l'étude du Système Aquifère du Sahara Septentrional SASS, Application à la nappe du Continental Intercalaire de la région Ouest du Sahara: Touat – Gourara – Tidikelt. Doctoral thesis, University of Ouargla, 237p.

Boualem, B., Egbueri, J.C., 2024. Graphical, statistical and index-based techniques integrated for identifying the hydrochemical fingerprints and groundwater quality of In Salah, Algerian Sahara. Environ Geochem Health 46, 158. https://doi.org/10.1007/s10653-024-01931-6.

Bouselsal, B., 2016. Etude hydrogéologique et hydrochimique de l'aquifère libre d'El Oued Souf SE Algérie. Thèse de doctorat. Université d'Annaba, Algérie, p. 204.

Bouselsal, B., 2017. Groundwater quality in arid regions: The case of Hassi Messaoud Region Se Algeria. Journal of Fundamental and Applied Sciences 91: 528.

Bouselsal, B., Saibi, S., 2022. Evaluation of groundwater quality and hydrochemical characteristics in the shallow aquifer of El-Oued Region Algerian Sahara. Groundwater for Sustainable Development 17:100747. https://doi.org/10.1016/j.gsd.2022.100747.

Bouselsal, B., Belksier, M.S., 2018. Caractérisation géochimique de l'aquifère de Complexe Terminal de El-Oued SE Algérie. Journal International Sciences et Technique de l'Eau et de l'Environnement. Volume III - Numéro 1 - Avril 2018. P 74 -80.

Bouselsal, B., Kherici, N., Hadj-Said, S., 2015. Vulnérabilité et risque de Pollution de la nappe libre d'El-Oued (SE Algérie) : application de la Méthode DRASTIC. Bulletin du Service Géologique National., Vol. 26, n° 1.

Boussaada, N., Bouselsal, B., Benhamida, S.A., Hammad, N., Kharroubi, M., 2023. Geochemistry and water quality assessment of continental intercalary aquifer in Ouargla region (Sahara, Algeria). Journal of Ecological Engineering 2023, 24(2), 279–294. https://doi.org/10.12911/22998993/156832.

Dhakate, R., More, S., Duvva, L.K. et al., 2023. Groundwater chemistry and health hazard risk valuation of fluoride and nitrate enhanced groundwater from a semi-urban region of South India. Environ Sci Pollut Res 30, 43554–43572. https://doi.org/10.1007/s11356-023-25287-z

Darling, W.G., Sorensen, J.P.R., Newell, A.J., Midgley, J., Benhamza, M., 2018. The age and origin of groundwater in the Great Western Erg Sub-Basin of the North-Western Sahara Aquifer

System: Insights from Krechba, Central Algeria. Applied Geochemistry 96:277–86. https://doi.org/10.1016/j.apgeochem.2018.07.010.

Egbueri, J.C., 2019. Groundwater quality assessment using pollution index of groundwater (PIG), ecological risk index (ERI) and hierarchical cluster analysis (HCA): A case study. Groundwater for Sustainable Development 10:100292. https://doi.org/10.1016/j.gsd.2019.100292.

Egbueri, J.C., Agbasi, J.C., Ayejoto, D.A., Khan, M.I., Khan, M.Y.A., 2023. Extent of anthropogenic influence on groundwater quality and human health-related risks: an integrated assessment based on selected physicochemical characteristics. Geocarto International 38(1):2210100. https://doi.org/10.1080/10106049.2023.2210100.

Farhat, S., Bali, M., Kamel, F., 2019. Geochemical and Statistical Studies of Mio-Pliocene Aquifer's Mineralization in Jerba Island, South-Eastern Tunisia. Physics and Chemistry of the Earth 111 (March): 35–52. https://doi.org/10.1016/j.pce.2019.03.006.

Foster, S.S.D., Lawrence, A.R., Morris, B.L., 1997. Groundwater in urban development: assessing management needs and formulating policy strategies. World Bank Technical Paper 390.

Freeze, R.A., Cherry, J.A., 1979. Groundwater. Prentice Hall, Inc, New Jersey.

Gleick, P.H., 2003. Global freshwater resources: Soft-path solutions for the 21st century. Science, Nov 28;302(5650):1524-8. doi: 10.1126/science.1089967.

Hammad, N., Bouselsal, B., Boussaada, N., Satouh, A., Lakhdari, A.S., 2023. Application of water quality index to assess the potability of the Phreatic Aquifer in Ouargla, Algeria. Ecological Engineering and Environmental Technology 24(5):36–45. https://doi.org/10.12912/27197050/163122.

Hao, C., Jiading, W., Fei, Z., Yaxing, Z., Chunying, X., 2022. Hydrochemical Characteristics and Formation Mechanisms of Groundwater in West Zoucheng City, Shandong Province, China. Environmental Monitoring and Assessment, 1–17. https://doi.org/10.1007/s10661-022-10136-2.

Haritash, A.K., Kaushik, C.P., Kanal, A., Kumar, Y.A., 2008. Suitability assessment of groundwater for drinking, irrigation and industrial use in some North Indian Villages. Environmental Monitoring and Assessment 145:397–406. https://doi.org/10.1007/s10661-007-0048-x.

Hill, R.A., 1940. Geochemical patterns in Coachella Valley. Trans. Am. Geophys. Union, Part I 21, 46–49. https://doi.org/10.1029/TR021i001p00046.

Houari, I.M., Bouselsal, B., Lakhdari, A.S. 2024., Evaluating Groundwater Potability and Health Risks from Nitrates in the Semi-Arid Region of Algeria. Ecological Engineering & Environmental Technology 2024, 25(6), 222–236. https://doi.org/10.12912/27197050/186954.

Karunanidhi, D., Aravinthasamy, P., Subramani, T., Deepak, K., Raj, S., 2021. Investigation of health risks related to multipath entry of groundwater nitrate using Sobol sensitivity indicators in an urban-industrial sector of south India. Environmental Research 200: 0013-9351.

Kaur, L., Rishi, M.S., Siddiqui, A.U., 2020. Deterministic and probabilistic health risk assessment techniques to evaluate non-carcinogenic human health risk (NHHR) due to fluoride

and nitrate in groundwater of Panipat Haryana, India. Environmental Pollution 259, 113711. https://doi.org/10.1016/j.envpol.2019.113711.

Kebili, M., Bouselsal, B., Gouaidia, L., 2021. Hydrochemical Characterization and Water Quality of the Continental Intercalary Aquifer in the Ghardaïa Region (Algerian Sahara). Journal of Ecological Engineering. 22(10), 152–162. https://doi.org/10.12911/22998993/142041.

Kharroubi, M., Bouselsal, B., Sudhir, K.S., 2024. Groundwater quality and non-carcinogenic element health risks assessment using multi-technical models: A case of the deep aquifer of the complex terminal in Ouargla city (southeastern Algeria). Groundwater for Sustainable Development 25 (2024) 101140. https://doi.org/10.1016/j.gsd.2024.101140.

Luo, W., Gao, X., Zhang, X., 2018. Geochemical processes controlling the groundwater chemistry and fluoride contamination in the Yuncheng Basin, China—An area with complex hydrogeochemical conditions. PLoS ONE 13(7): e0199082.

Mahanty, B., Lhamo, P., Sahoo, N.K., Monte Carlo, 2023. Science of the Total Environment Inconsistency of PCA-Based Water Quality Index – Does It Reflect the Quality? Science of the Total Environment 866 (October 2022): 161353. https://doi.org/10.1016/j.scitotenv.2022.161353.

Massuel, S., George, B.A., Venot, J.P., Bharati, L., Acharya, S., 2013. Improving assessment of groundwater-resource sustainability with deterministic modelling: a case study of the semi-arid Musi sub-basin, South India. Hydrogeology Journal 21(7):1567-1580.

Mudgal, K.D., Kumari, M., Sharma, D.K., 2009. Hydrochemical analysis of drinking water quality of Alwar District, Rajasthan. Natural Sciences 7(2):30–39.

Obeidat, M.M., Awawdeh, M., Al-Rub, F.A., Al-Ajlouni, A., 2012. An innovative nitrate pollution index and multivariate statistical investigations of groundwater chemical quality of Umm Rijam Aquifer B4, North Yarmouk River Basin, Jordan. In Vouddouris, K., Voutsa, D. (Eds.), Water Quality Monitoring and Assessment. Croatia: InTech, pp. 169-188. https://doi.org/10.5772/32436.

Ouarekh, M., Bouselsal, B., Belksier, M.S., Benaabidate, L., 2021. Water quality assessment and hydrogeochemical characterization of the Complex Terminal aquifer in Souf valley, Algeria. Arabian Journal of Geosciences, 14, 2239. https://doi.org/10.1007/s12517-021-08498-x.

Panneerselvam, B., Karuppannan, S., Muniraj, K., 2021. Evaluation of drinking and irrigation suitability of groundwater with special emphasizing the health risk posed by nitrate contamination using nitrate pollution index (NPI) and human health risk assessment (HHRA). Human and Ecological Risk Assessment: An International Journal 27(5):1324–1348. https://doi.org/10.1080/10807039.2020.1833300

Piper, A.M., 1944 Graphical interpretation of water analysis. Transactions of the American Geophysical Union., 25:914 -923.

Ramesh, K., Soorya, V., 2012. Hydrochemical analysis and evaluation of groundwater quality in and around Hosur, Krishnagiri District, Tamil Nadu, India. International Journal of Research in Chemistry and Environment 2(3):13–122.

Sahu, P., Kisku, G.C., Singh, P.K., Kumar, V., Kumar, P., Shukla, N., 2018. Multivariate statistical interpretation on seasonal variations of fluoride-contaminated groundwater quality of Lalganj Tehsil, Raebareli District, UP, India. Environmental Earth Sciences. https://doi.org/10.1007/s12665-018-7658-1

Sawyer, C.N., McCarty, P.L., 1967. Chemistry for Sanitary Engineers, 2nd edn. McGraw-Hill, New York, p. 518.

Schoeller, H., 1965. Qualitative evaluation of groundwater resources. In Methods and Techniques of Groundwater Investigations and Development. UNESCO, 5483.

Sengupta, P., 2013. Potential health impacts of hard water. International Journal of Preventive Medicine 4(8):866–875.

Shaikh, H., Gaikwad, H., Kadam, A., et al., 2020. Hydrogeochemical characterization of groundwater from semiarid region of western India for drinking and agricultural purposes with special reference to water quality index and potential health risks assessment. Applied Water Science 10:204. https://doi.org/10.1007/s13201-020-01287-z

Spalding, R.F., Exner, M.E., 1993. Occurrence of nitrate in groundwater - a review. Journal of Environmental Quality 22:392-402.

Subba Rao, N., 2021. Spatial distribution of quality of groundwater and probabilistic non-carcinogenic risk from a rural dry climatic region of South India. Environmental Geochemistry and Health 43, 971–993. https://doi.org/10.1007/s10653-020-00621-3.

Subba Rao, N., Maya, C., 2019. Hydrogeochemical processes regulating the spatial distribution of groundwater contamination, using pollution index of groundwater (PIG) and hierarchical cluster analysis (HCA): A case study. Groundwater for Sustainable Development 9:100238.

Subba Rao, N., 2012. PIG: a numerical index for dissemination of groundwater contamination zones. Hydrological Processes 26, 3344–3350.

Tawfeeq, J.MS., Dişli, E. & Hamed, M.H., 2024. Hydrogeochemical evolution processes, groundwater quality, and non-carcinogenic risk assessment of nitrate-enriched groundwater to human health in different seasons in the Hawler (Erbil) and Bnaslawa Urbans, Iraq. Environmental Science and Pollution Research 31, 26182–26203. https://doi.org/10.1007/s11356-024-32715-1 https://doi.org/10.1007/s11356-024-32715-1.

Touahri, M., Belksier, M.S., Bouselsal, B., Kebili, M., 2022. Groundwater Quality Assessment of Hassi Messaoud Region (Algerian Sahara). Journal of Ecological Engineering, 23(11), 165–178. https://doi.org/10.12911/22998993/153396.

UNESCO, 2012. World's groundwater resources are suffering from poor governance. UNESCO Natural Sciences Sector News, Paris, Natural Sciences Sector News.

USEPA, 2001. Baseline Human Health Risk Assessment Vasquez Boulevard and I-70 Superfund Site, Denver, CO. http://www.epa.gov/region8/superfund/sites/VB-170-Risk.pdf.

USEPA, 1989. Risk Assessment Guidance for Superfund, Volume 1: Human Health Evaluation Manual (Part A) (EPA/540/1–89/002: Interim Final). Washington DC: Office of Emergency and Remedial Response.

Verma, A., Singh, N.B., 2021. Evaluation of Groundwater Quality Using Pollution Index of Groundwater (PIG) and Non-Carcinogenic Health Risk Assessment in Part of the Gangetic Basin. Acta Geochimica 40(3): 419–40. https://doi.org/10.1007/s11631-020-00446-y.

WHO, 2017. World Health Statistics 2017: Monitoring Health for the SDGs, Sustainable Development Goals. Geneva: World Health Organization; 2017. License: CC BY-NC-SA 3.0 IGO.

Zhang, C., Li, X., Hou, X., et al., 2023. Characterization of drinking groundwater quality and assessment of human health risk in Xin'an Spring Basin, a typical mining and karst area of northern China. Environmental Earth Sciences 82, 282. https://doi.org/10.1007/s12665-023-10994-0.